Intranasal MSC-derived A1-exosomes ease inflammation, and prevent abnormal neurogenesis and memory dysfunction after status epilepticus

Qianfa Long[a,1,2], Dinesh Upadhya[a,b,c,2,3], Bharathi Hattiangady[a,b,c], Dong-Ki Kim[a], Su Yeon An[a], Bing Shuai[a,b,c], Darwin J. Prockop[a,c,d,4,5], and Ashok K. Shetty[a,b,c,4,5]

[a]Institute for Regenerative Medicine, Texas A&M Health Science Center College of Medicine, Temple, TX 76502; [b]Olin E. Teague Veterans' Medical Center, Central Texas Veterans Health Care System, Temple, TX 76502; [c]Department of Molecular and Cellular Medicine, Texas A&M Health Science Center College of Medicine, College Station, TX 77843; and [d]Department of Clinical Translational Medicine, Texas A&M Health Science Center College of Medicine, College Station, TX 77843

Contributed by Darwin J. Prockop, March 13, 2017 (sent for review December 23, 2016; reviewed by Cesar Borlongan and Daniel A. Peterson)

Status epilepticus (SE), a medical emergency that is typically terminated through antiepileptic drug treatment, leads to hippocampus dysfunction typified by neurodegeneration, inflammation, altered neurogenesis, as well as cognitive and memory deficits. Here, we examined the effects of intranasal (IN) administration of extracellular vesicles (EVs) secreted from human bone marrow-derived mesenchymal stem cells (MSCs) on SE-induced adverse changes. The EVs used in this study are referred to as A1-exosomes because of their robust antiinflammatory properties. We subjected young mice to pilocarpine-induced SE for 2 h and then administered A1-exosomes or vehicle IN twice over 24 h. The A1-exosomes reached the hippocampus within 6 h of administration, and animals receiving them exhibited diminished loss of glutamatergic and GABAergic neurons and greatly reduced inflammation in the hippocampus. Moreover, the neuroprotective and antiinflammatory effects of A1-exosomes were coupled with long-term preservation of normal hippocampal neurogenesis and cognitive and memory function, in contrast to waned and abnormal neurogenesis, persistent inflammation, and functional deficits in animals receiving vehicle. These results provide evidence that IN administration of A1-exosomes is efficient for minimizing the adverse effects of SE in the hippocampus and preventing SE-induced cognitive and memory impairments.

status epilepticus | memory dysfunction | neuroinflammation | exosomes | adult neurogenesis

Status epilepticus (SE) is a grave medical crisis that requires swift remedy through all age groups (1, 2). It can produce substantial neurodegeneration, blood–brain barrier disruption, and inflammation in the hippocampus if not extinguished quickly by antiepileptic drug (AED) treatment (3–5). An episode of extended SE is sufficient to cause chronic hippocampus dysfunction, exemplified by persistent inflammation with activation of microglia and monocyte infiltration, loss of sizable fractions of several subclasses of inhibitory interneurons, aberrant and waned neurogenesis, hippocampus-dependent cognitive and memory impairments, and chronic epilepsy (5–12). Numerous situations such as head trauma, stroke, Alzheimer's disease, brain tumor, and encephalitis can engender SE. Although administration of AEDs leads to termination of SE in most instances, it does not thwart the evolution of SE into chronic epilepsy (13–16). A multitude of changes ensue in the hippocampus after an episode of SE, which evolve over a period of months, years, or even decades, and result in chronic epilepsy when they have reached certain thresholds (11, 17, 18). Hence, there is an urgent need to find an adjuvant therapy with AEDs that not only provides neuroprotection and suppression of inflammation in the early phase after SE but also maintains normal neurogenesis, preserves cognitive and memory function, and thwarts epilepsy development in the chronic phase after SE. The i.v. administration of bone marrow-derived mononuclear cells (MNCs) or mesenchymal stem cells (MSCs) has shown potential for modulating SE-induced adverse effects in the hippocampus and reducing the severity of chronic epilepsy (19). However, clinical therapies with MNCs or MSCs face considerable challenges in regard to the variable biological activity of different preparations of the cells and the logistics of delivering the cells to the bedside or emergency room.

A feasible alternative would be the dispensation of prebanked extracellular vesicles (EVs) generated from MSCs, as human MSC (hMSC)-derived EVs seemed to have most of the antiinflammatory and neuroprotective activity of MSCs (20). Moreover, several studies suggest that therapeutic benefits of MSC administration are largely explained by paracrine effects mediated by soluble factors or EVs secreted by MSCs (21–24). Furthermore, EVs can cross the blood–brain barrier and deliver various therapeutic factors to the brain (25, 26). EVs containing a multitude of mRNAs, miRNAs, and proteins (26, 27) can be harvested, characterized, and banked from MSCs obtained from

Significance

This study demonstrated that intranasal (IN) administration of A1-exosomes alleviates multiple adverse changes that typically emerge after status epilepticus (SE), a medical crisis that presents a high propensity to evolve into chronic hippocampus dysfunction. Specifically, A1-exosome treatment after SE led to reduced neuron loss and inflammation, maintenance of normal neurogenesis, and preservation of cognitive and memory function. The results have significance for clinical application of A1-exosomes for curbing the evolution of SE-induced injury into chronic hippocampus dysfunction. The results also imply that IN administration of A1-exosomes is therapeutic for other neurological conditions that present with significant neuroinflammation.

Author contributions: Q.L., D.U., B.H., D.J.P., and A.K.S. designed research; Q.L., D.U., B.H., D.-K.K., S.Y.A., and B.S. performed research; D.-K.K. and S.Y.A. contributed new reagents/analytic tools; Q.L., D.U., B.H., D.J.P., and A.K.S. analyzed data; and Q.L., D.U., B.H., D.J.P., and A.K.S. wrote the paper.

Reviewers: C.B., Center of Excellence for Aging and Brain Repair University of South Florida; and D.A.P., Rosalind Franklin University of Medicine and Science.

The authors declare no conflict of interest.

Freely available online through the PNAS open access option.

[1]Present address: Department of Neurosurgery, Xi'an Central Hospital, School of Medicine, Xi'an Jiao Tong University, Xi'an 710003, P.R. China.

[2]Q.L. and D.U. contributed equally to this work.

[3]Present address: Center for Molecular Neurosciences, Manipal University, Manipal 576104, Karnataka, India.

[4]D.J.P. and A.K.S. contributed equally to this work.

[5]To whom correspondence may be addressed. Email: prockop@medicine.tamhsc.edu or shetty@medicine.tamhsc.edu.

This article contains supporting information online at www.pnas.org/lookup/suppl/doi:10.1073/pnas.1703920114/-/DCSupplemental.

several sources such as bone marrow, lipoaspirate of liposuction procedures, umbilical cord, and human-induced pluripotent stem cells (28–30). The use of EVs also avoids several potential safety hazards such as the risk of tumors. Besides, EVs have several distinct advantages over cells for use in clinical therapies. Their compositions can be defined and standardized because they are stable and not responsive to external stimuli. EVs can be made readily available for use in patients, as they are far more stable to freezing and thawing. Also, if the small size of EVs makes it possible to administer them via an IN route, they may be broadly applicable as a noninvasive therapy.

Therefore, we rigorously ascertained the efficacy of IN administration of EVs derived from human bone marrow-derived MSCs by using a pilocarpine model of SE in mice. The EVs used in this study have been well characterized and are referred to as A1-exosomes because of their robust antiinflammatory properties (20). First, we measured the ability of IN administered A1-exosomes to enter the hippocampus, suppress inflammation, and protect glutamatergic and GABAergic neurons in the early phase after SE. Next, we measured the proficiency of IN-administered A1-exosomes for maintaining normal neurogenesis and cognitive and memory function with persistent suppression of inflammation in the chronic phase after SE.

Results

Preparation, Selection and Characterization of A1-Exosomes from Human Bone Marrow-Derived MSCs. The generation, isolation, and capture of EVs of uniform size (80–100 nm in diameter) from human bone marrow-derived MSCs were performed as detailed in our recent report (20). The EVs generated through this procedure were positive for classical EV markers such as CD63 and CD81 but negative for CD9 and 13 other epitopes found on the surface of MSCs. Each batch of EVs was also tested for antiinflammatory activity in the spleen by using a model of systemic inflammation induced by administration of LPS. Only EVs that exhibited antiinflammatory activity in the spleen were labeled as A1-exosomes and used in the SE model. Further details are provided in *SI Materials and Methods*.

IN-Dispensed A1-Exosomes Incorporated into Cortical and Hippocampal Neurons. We investigated whether IN administration of A1-exosomes after SE would result in targeting of these exosomes into the hippocampus, the region exhibiting intense hyperactivity of neurons, increased oxidative stress, and inflammation with infiltration of peripheral monocytes during and/or after SE (5, 12). We administered PKH26-labeled A1-exosomes via IN route (15 μg, ~7.5×10^9) immediately after the termination of 2 h of SE by an injection of diazepam. Six hours later, animals were perfused ($n = 4$), and serial sections through the entire brain were processed for immunofluorescence by using markers of neurons (neuronal nuclear antigen [NeuN]), astrocytes (GFAP), and microglia (IBA-1) and *Z*-sectioning in a confocal microscope. We found red-colored PKH26$^+$ particles (i.e., A1-exosomes) throughout the olfactory bulb, frontoparietal cortex, basal forebrain, striatum, and dorsal hippocampus. At dorsal hippocampal levels, most exosomes were in small clusters and were seen within the cytoplasm of neurons or attached to the cell membrane of neurons (Fig. 1 *A1–C2*). In the hippocampus, exosomes were clearly seen within dentate hilar neurons (Fig. 1 *B1* and *B2*) and the CA3 pyramidal neurons (Fig. 1 *C1* and *C2*). Occasionally, exosomes were also found in the cytoplasm of dentate granule cells (Fig. 1 *B1* and *B2*) and the CA1 pyramidal neurons. We also examined their presence within GFAP$^+$ astrocytes (Fig. *1D*) and IBA-1$^+$ microglial cells (Fig. 1*E*) in the hippocampus. None were seen in the cell body of astrocytes but were found inside the cell body of some microglia. However, exosomes were frequently seen in close proximity to astrocyte and microglial processes. In rostral regions of the cerebral cortex, accumulation of exosomes could be seen in virtually all neurons and a vast majority of microglia (Figs. S1 and S2). Exosomes were also seen in close proximity to processes of astrocytes and microglia. Interestingly, whereas neurons displayed isolated or smaller clusters of exosomes, a greater fraction of microglia displayed larger clusters of exosomes within their cytoplasm (Fig. S2). Thus, within 6 h of IN administration, A1-exosomes incorporated robustly into neurons and microglia in rostral regions of the cerebral cortex, and predominantly into neurons in the cortex and the hippocampus at dorsal hippocampal levels.

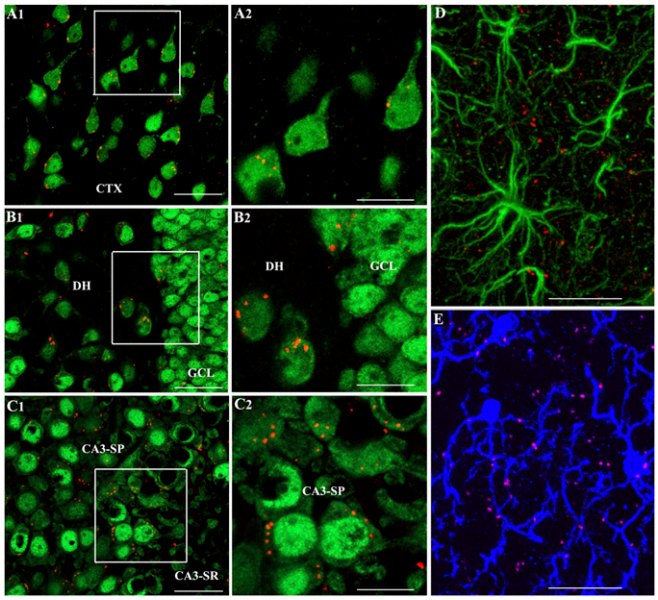

Fig. 1. A1-exosomes invade the frontoparietal cerebral cortex and the dorsal hippocampus within 6 h after IN administration. (*A1–C2*) The presence of PKH26$^+$ exosomes (red dots) within the cytoplasm or in close contact with the cell membrane of NeuN$^+$ neurons in the cerebral cortex (*A1*), the DH and GCL (*B1*), and CA3 pyramidal neurons (*C1*) of the hippocampus at 6 h after their IN administration. (*A2*, *B2*, and *C2*) Magnified views of boxed regions in *A1*, *B1*, and *C1*. (*D*) Lack of exosomes within the soma of GFAP$^+$ astrocytes and the presence of some exosomes adjacent to astrocyte processes. (*E*) Presence of exosomes within the soma or processes of some IBA-1$^+$ microglia. CA3-SP, CA3 stratum pyramidale; CA3-SR, CA3 stratum radiatum; CTX, cortex. (Scale bars: *A1*, *B1*, and *C1*, 50 μm; *A2*, *B2*, and *C2*, 25 μm; *D* and *E*, 25 μm.)

IN Delivery of A1-Exosomes After SE Prevented the Rise of Multiple Proinflammatory Cytokines and Increased the Concentration of Some Antiinflammatory Cytokines and Growth Factors in the Hippocampus. We measured 24 cytokines in hippocampal lysates obtained from animals belonging to different groups ($n = 6$ per group) at 24 h post-SE by using 96-well array plates that were precoated with specific cytokine capture antibodies. Sixteen proinflammatory cytokines exhibited up-regulation in animals receiving vehicle after SE (SE-VEH group) in comparison with naive control animals (Table S1). Among these, the concentrations of seven proinflammatory cytokines was significantly reduced in animals receiving A1-exosomes after SE (SE-EVs group; Fig. 2 *A–G*) in comparison with animals in the SE-VEH group. These include TNF-α, IL-1β, monocyte chemoattractant protein-1 (MCP-1), stem cell factor (SCF), macrophage inflammatory protein-1α (MIP-1α), GM-CSF, and IL-12. Animals in the SE-EVs group also displayed enhanced concentrations of antiinflammatory cytokine IL-10 (Fig. 2*H*), granulocyte colony-stimulating factor (G-CSF; Fig. 2*I*), platelet-derived growth factor-β (PDGF-β, Fig. 2*J*), IL-6 (Fig. 2*K*), and IL-2 (Fig. 2*L*). As TNF-α and IL-1β are among the major proinflammatory cytokines that are implicated in brain diseases exhibiting inflammation and/or cognitive and

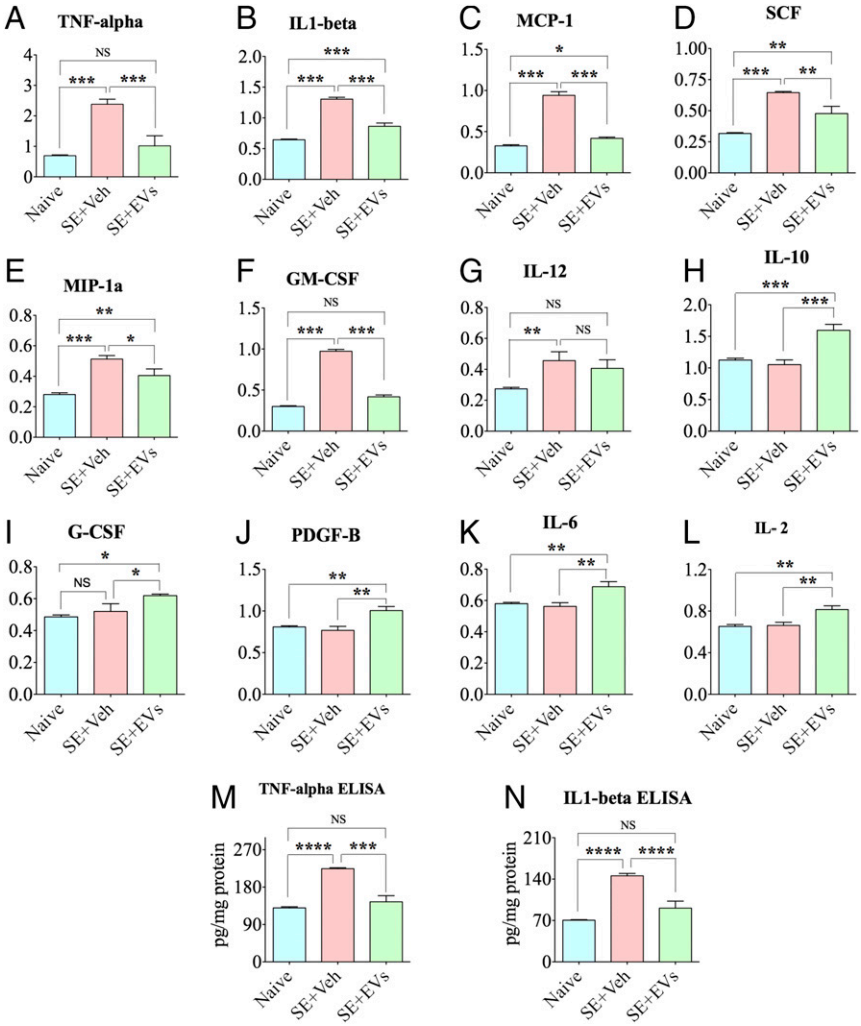

Fig. 2. IN administration of A1-exosomes 2 h after SE eases inflammation in the hippocampus when examined 24 h post-SE. Bar charts compare the relative concentrations of multiple cytokines between naive control animals, SE+VEH animals, and SE+EVs animals. Assays were by multiplexed ELISAs. Animals in the SE+VEH group display increased concentration of proinflammatory cytokines TNF-α, IL-1β, MCP-1, SCF, MIP-1α, GM-CSF, and IL-12 (*A–G*), whereas animals in the SE+EVs group exhibit significantly reduced concentrations of these cytokines. This group also showed increased concentration of antiinflammatory cytokines and growth factors such as IL-10, G-CSF, PDGF-β, IL-6, and IL-2 (*H–L*). Bar charts in *M* and *N* compare levels of TNF-α and IL-1β in the hippocampus measured through independent ELISAs. In comparison with naive controls, the concentrations of these proinflammatory cytokines are increased in the SE+VEH group but normalized in the SE+EVs group (*$P <$ 0.05, **$P < 0.01$, ***$P < 0.001$, and ****$P < 0.0001$).

memory dysfunction and have proconvulsive properties (31), we further confirmed their concentration through independent quantitative ELISAs. The results clearly showed their upregulation at 24 h post-SE in animals in the SE-VEH group and normalized levels in the SE-EVs group (Fig. 2 *M* and *N*). Thus, IN administration of A1-exosomes commencing 2 h post-SE was adequate for greatly easing the inflammatory storm triggered by SE.

IN Delivery of A1-Exosomes After SE Greatly Reduced the Activation of Microglia in the Hippocampus. We measured the extent of inflammation in the hippocampus at 4 d post-SE in animals receiving vehicle or A1-exosomes through immunohistochemical staining of serial sections for ED-1 (CD68, a marker of activated microglia or macrophages in the brain) and stereological quantification of ED-1$^+$ cells in the dentate gyrus (DG) and CA1 and CA3 subfields of the hippocampus ($n = 5$–6 per group; Fig. 3 *A1–E*). Animals in the SE-VEH group exhibited increased density of ED-1$^+$ microglia, with several morphological changes, particularly in the CA1 and CA3 subfields. A fraction of microglia exhibited hypertrophy of soma with multiple short processes whereas some others exhibited round or oval-shaped soma with no or minimal processes, both of which are characteristics of activated microglia (Fig. 3 *A2* and *A3*). In contrast, animals in the SE-EVs group exhibited not only reduced density of ED-1$^+$ microglia but also a greatly diminished intensity of ED-1 staining (Fig. 3 *B1–B3*). Stereological quantification confirmed reduced numbers of ED-1$^+$ microglia in the DG (Fig. 3*C*), CA1 and CA3 subfields (Fig. 3*D*), and in the entire hippocampus (Fig. 3*E*). The reductions were 50% for the DG, 72% for the CA1 and CA3 subfields, and 66% for the entire hippocampus ($P < 0.05$–0.01; Fig. 3 *C–E*).

IN Delivery of A1-Exosomes After SE Reduced the Overall Loss of Neurons in the Dentate Hilus and the CA1 Cell Layer of the Hippocampus. SE typically causes degeneration of neurons in certain regions/layers of the hippocampus. To ascertain the extent of SE-induced neurodegeneration in the hippocampus of animals receiving vehicle or A1-exosomes after SE, we performed NeuN immunostaining of serial sections through the entire hippocampus at 4 d post-SE (Fig. 4 *A1–C3*). In comparison with naive control animals, the SE-VEH and SE-EVs groups showed reduced densities of neurons in the dentate hilus (DH) and the CA1 pyramidal cell layer but no discernable changes in the granule cell layer (GCL) and the CA3 pyramidal cell layer ($n = 5$–6 per group; Fig. 4 *A1–C3*). Stereological quantification revealed that the overall neuron loss in the DH and CA1 cell layer ranged from 40% to 47% in the SE-VEH group ($P < 0.001$) and from 25% to 26% in the SE-EVs group ($P < 0.01$–0.001). Because of neuroprotection mediated by A1-exosomes, animals in the SE-EVs group displayed a 30–41% greater number of neurons than animals in the SE-VEH group ($P < 0.01$–0.001; Fig. 4 *D* and *E*). Thus, IN administration of A1-exosomes after

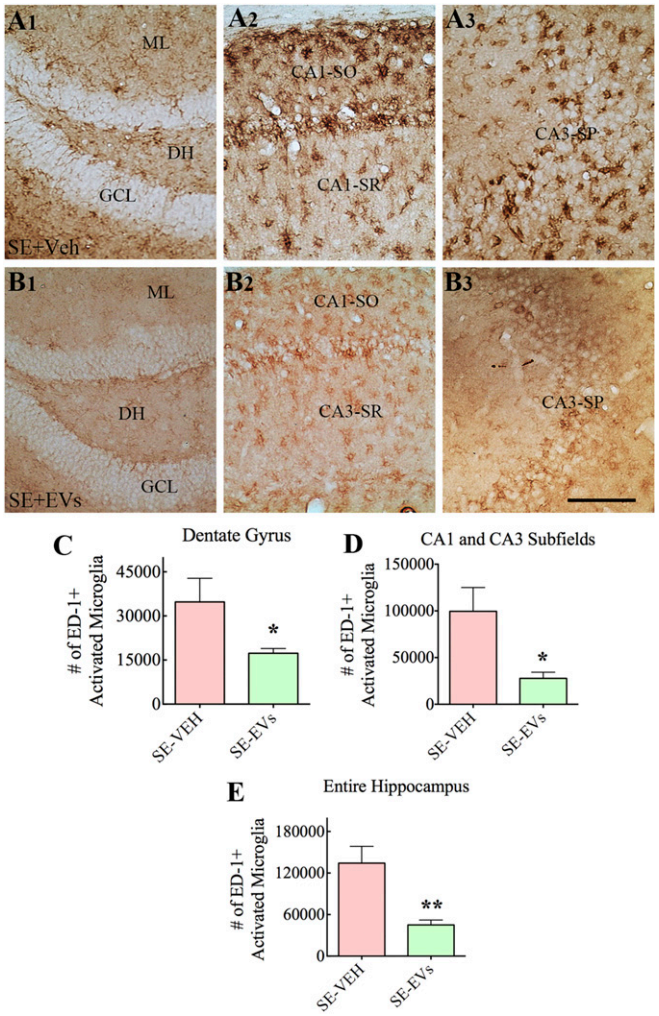

Fig. 3. IN administration of A1-exosomes 2 h after SE greatly reduces the density of ED-1$^+$ (CD68$^+$) activated microglia in the hippocampus when examined 4 d post-SE. (*A1–B3*) Distribution of ED-1$^+$ activated microglia in the DG (*A1* and *B1*), the CA1 subfield (*A2* and *B2*), and the CA3 subfield (*A3* and *B3*) of an animal in the SE-VEH group (*A1–A3*) and an animal in the SE-EVs group (*B1–B3*). ML, molecular layer; SO, stratum oriens; SP, stratum pyramidale; SR, stratum radiatum. Bar charts in *C–E* compare the numbers of ED-1$^+$ microglia in the DG (*C*), CA1 and CA3 subfields (*D*), and the entire hippocampus (*E*). Note that animals receiving A1-exosomes (i.e., SE-EVs group) display reduced numbers of ED-1$^+$ activated microglia compared with animals in the SE-VEH group (*$P < 0.05$ and **$P < 0.01$). (Scale bar: 100 μm.)

SE reduced the loss of neurons in regions of the hippocampus that are highly susceptible to SE-induced neurodegeneration.

IN Delivery of A1-Exosomes After SE Restrained the Loss of Several Subclasses of Inhibitory Interneurons in the Hippocampus. Several subclasses of inhibitory GABAergic interneurons in the hippocampus are highly susceptible to SE. To measure the extent of SE-induced loss of inhibitory interneurons in animals receiving vehicle or A1-exosomes after SE, we performed immunostaining of serial sections through the entire hippocampus for the calcium binding protein parvalbumin (PV), and neuropeptides somatostatin (SS) and neuropeptide Y (NPY) at 4 d post-SE (n = 5–6 per group). The interneurons positive for PV displayed reduced density in the DH-GCL region and the CA1 subfield after SE (Fig. 4 *F1–H3*). Stereological measurement demonstrated that the overall PV$^+$ interneuron loss in the DH-GCL and the CA1 subfield varied from 43% to 56% in the SE-VEH group ($P < 0.001$) and from 24% to 25% in the SE-EVs group ($P <$ 0.01–0.001). Because of the protection mediated by A1-exosomes, the SE-EVs group displayed 34–69% greater numbers of PV$^+$ interneurons than the SE-VEH group ($P < 0.05$; Fig. 4 *I* and *J*). Interneurons expressing SS exhibited reduced densities in the DH+GCL, CA1, and CA3 regions after SE (Fig. 5 *A1–C3*). Stereological cell counting showed that the overall SS$^+$ interneuron loss in these regions ranged from 39% to 44% in the SE-VEH group ($P <$ 0.01–0.001). In contrast, the SE-EVs group displayed no significant loss in the DH+GCL region and the CA1 subfield ($P > 0.05$) but a 27% loss in the CA3 subfield ($P <$ 0.05). In comparison with the SE-VEH group, the SE-EVs group displayed 47–52% greater numbers of SS$^+$ interneurons in the DH+GCL and CA1 regions ($P < 0.01$; Fig. 5 *D* and *E*) and a 20% higher number in the CA3 subfield ($P > 0.05$; Fig. 5F). The interneurons positive for NPY displayed reduced density only in the DH-GCL region after SE (Fig. 5 *G1–I3*). Stereological quantification revealed that the NPY$^+$ interneuron loss in the DH+GCL region is 46% in the SE-VEH group and 35% in the SE-EVs group ($P < 0.01$; Fig. 5*J*). In comparison with the SE-VEH group, the SE-EVs group displayed 22% higher numbers of NPY$^+$ interneurons ($P > 0.05$; Fig. 5*J*). Thus, IN administration of A1-exosomes after SE diminished the loss of several subclasses of GABAergic interneurons in the hippocampus.

IN Delivery of A1-Exosomes After SE Averted Cognitive and Memory Impairments in the Chronic Phase. Cognitive and memory impairments typically ensue after SE. We examined animals 5–6 wk after SE with vehicle or A1-exosome treatment via three distinct behavioral tests. These include an object location test (OLT), a novel object recognition test (NORT), and a pattern separation test (PST; n = 8–10 per group). We first measured the cognitive ability of animals through an OLT. The choice to explore an object displaced to a novel location in this test reflects the ability of the animal to discern minor changes in its immediate environment (Fig. 6*A1*). Maintenance of this function depends on the integrity of the hippocampus circuitry (32). Animals in the SE-VEH group were impaired, as they did not show affinity for the object moved to a novel place (Fig. 6*A3*). Rather, they spent nearly equal amounts of time with the object in the familiar place and the object in the novel place ($P >$ 0.05). In contrast, animals belonging to the SE-EVs group showed a greater affinity for exploring the novel place object (NPO) over the familiar place object (FPO; $P < 0.01$; Fig. 6*A4*), which matched the normal behavior typically observed in naive control animals ($P < 0.0001$; Fig. 6*A2*). As animals belonging to different groups explored objects for comparable durations ($P >$ 0.05; Fig. 6*A5*) in the testing phase, the results were not influenced by variable object exploration times between groups. Thus, SE causes hippocampus-dependent cognitive dysfunction, but early intervention with A1-exosomes prevents this impairment.

We next examined recognition memory function by using a NORT. Recognition memory function depends on the integrity of the perirhinal cortex and the hippocampus. We examined animals with a 15-min delay between the "object exploration phase" comprising the exploration of two identical objects for 5 min in an arena and the "testing phase" involving the exploration of objects in the same arena but with replacement of one of the objects with a new object (Fig. 6*B1*) (32). Animals belonging to the SE-VEH group showed an inability of novel object (NO) discrimination, as they spent similar percentages of time exploring the familiar object (FO) and the NO ($P >$ 0.05; Fig. 6*B3*). However, animals in the SE-EVs group spent greater percentages of their object exploration time with the NO ($P < 0.0001$; Fig. 6*B4*), akin to that observed in naive control animals ($P < 0.0001$; Fig. 6*B2*). Again, animals in all groups explored objects for comparable durations ($P > 0.05$;

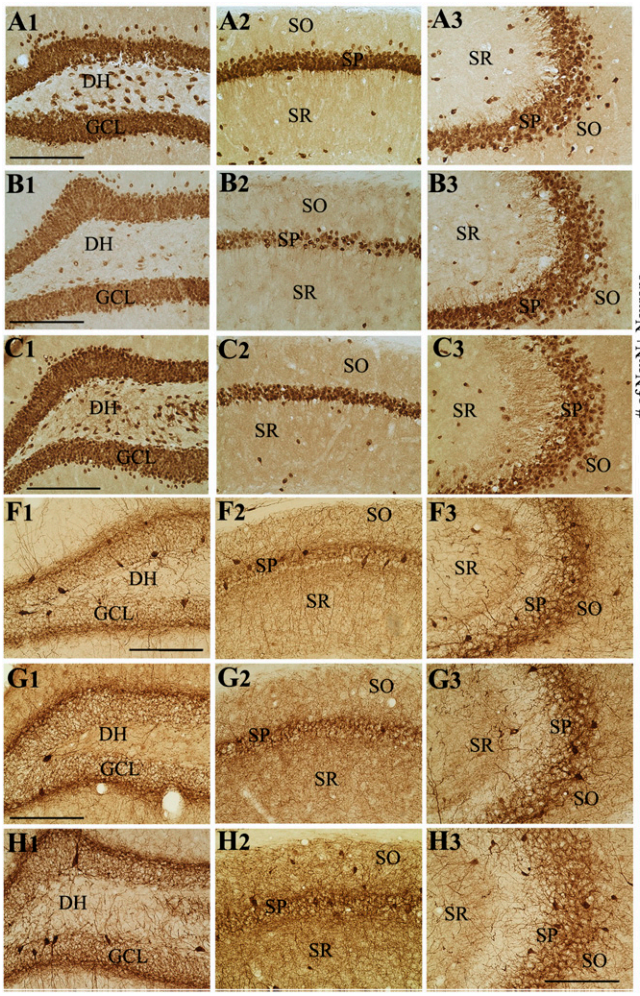

Fig. 4. IN administration of A1-exosomes 2 h after SE reduces the loss of NeuN$^+$ neurons and PV$^+$ interneurons in the DG and the CA1 subfield when examined 4 d post-SE. (*A1–C3*) Distribution of NeuN$^+$ neurons in the DG (*A1*, *B1*, and *C1*), the CA1 subfield (*A2*, *B2*, and *C2*), and the CA3 subfield (*A3*, *B3*, and *C3*) of a naive control mouse (*A1–A3*), a mouse in the SE-VEH group (*B1–B3*), and a mouse in the SE-EVs group (*C1–C3*). Bar charts in *D* and *E* compare the numbers of NeuN$^+$ neurons in the DH (*D*) and the CA1 pyramidal cell layer (*E*) of the hippocampus. Although both SE groups display reduced numbers of NeuN$^+$ neurons in comparison with the naive control group, the SE-EVs group exhibits greater numbers of surviving neurons than the SE-VEH group, implying neuroprotection after IN administration of A1-exosomes. (*F1–H3*) Distribution of PV$^+$ interneurons in the DG (*F1*, *G1*, and *H1*), the CA1 subfield (*F2*, *G2*, and *H2*), and the CA3 subfield (*F3*, *G3*, and *H3*) of a naive control mouse (*F1–F3*), a mouse from the SE-VEH group (*G1–G3*), and a mouse from the SE-EVs group (*H1–H3*). Bar charts in *I* and *J* compare the numbers of PV$^+$ interneurons in the DH+GCL (*I*) and the CA1 subfield (*J*) of the hippocampus. Although both SE groups display reduced numbers of PV$^+$ interneurons in the DH+GCL and CA1 subfield in comparison with the naive control group, the SE-EVs group exhibits greater numbers of PV$^+$ interneurons than the SE-VEH group, implying protection of these interneurons after IN administration of A1-exosomes. SO, stratum oriens, SP, stratum pyramidale; SR, stratum radiatum (*$P < 0.05$; **$P < 0.01$; ***$P < 0.001$). (Scale bar: 200 μm.)

Fig. 6*B5*) in the testing phase. These results demonstrated that A1-exosome treatment after SE prevents recognition memory impairment.

Following the aforementioned cognitive and memory tests, we further investigated the ability of animals for pattern separation by using an PST, a relatively complex test for discriminating analogous experiences through storage of similar representations in a nonoverlapping manner (33, 34). In this test, each animal successively explored two different sets of identical objects (object types 1 and 2) placed on distinct types of floor patterns (patterns 1 and 2 [P1 and P2]) for 5 min each in the two acquisition trials separated by 15 min (Fig. 6*C1*). Fifteen minutes later, in the testing phase (trial 3), each animal explored an object from trial 2 (which is now an FO) and an object from trial 1 (which is now an NO) placed on the floor pattern used in trial 2 (i.e., P2). Excellent pattern separation ability in naive animals was revealed by a greater exploration of the object from trial 1 (i.e., NO on P2) than the object from trial 2 (i.e., FO on P2; $P < 0.0001$; Fig. 6*C2*). In contrast, animals belonging to the SE-VEH group showed no preference for the NO on P2, as they spent nearly similar amounts of time with the NO and the FO on P2 ($P > 0.05$; Fig. 6*C3*), implying an impaired ability for pattern separation. However, animals in the SE-EVs group spent greater percentages of their object exploration time with the NO ($P < 0.0001$; Fig. 6*C4*), like the behavior seen in naive control animals ($P < 0.0001$; Fig. 6*C2*). These findings were not influenced by variable object exploration times between groups, as animals belonging to different groups explored objects for comparable durations ($P > 0.05$; Fig. 6*C5*). Thus, A1-exosome treatment rescues animals from developing SE-induced pattern separation dysfunction.

IN Delivery of A1-Exosomes After SE Promoted Normal Hippocampal Neurogenesis in the Chronic Phase. Hippocampal neurogenesis exhibits a biphasic response to SE, with increased and abnormal neurogenesis in the early phase and persistently declined neurogenesis in the chronic phase (6, 7). We investigated the effects of IN administration of A1-exosomes after SE on long-term neurogenesis in the hippocampus (i.e., 6 wk after SE; $n = 6$ per group). In comparison with naive controls (Fig. 7 *A1* and *A2*), animals in SE-VEH group exhibited decreased neurogenesis ($P < 0.0001$; Fig. 7 *B1* and *B2*), whereas animals in the SE-EVs group (Fig. 7 *C1* and *C2*) displayed a pattern and extent of neurogenesis that is equivalent to age-matched naive control animals ($P > 0.05$) and a greater extent of neurogenesis than animals in the SE-VEH group ($P < 0.01$; Fig. 7*D*). Furthermore, SE-VEH animals showed significant loss of dentate hilar neurons positive for reelin, a protein important for directing the migration of newly born neurons in the subgranular zone (SGZ) to the GCL ($P < 0.01$; Fig. 7 *E–H*). Interestingly, reelin$^+$ positive neuron numbers in the SE-EVs group were comparable to those in naive control animals ($P > 0.05$; Fig. 7 *E–H*) and greater than in the SE-VEH group ($P < 0.05$). To determine the extent of abnormal migration of newly born granule cells into the DH, we quantified the numbers of neurons positive for prox-1 (a marker of dentate granule cells) in the DH

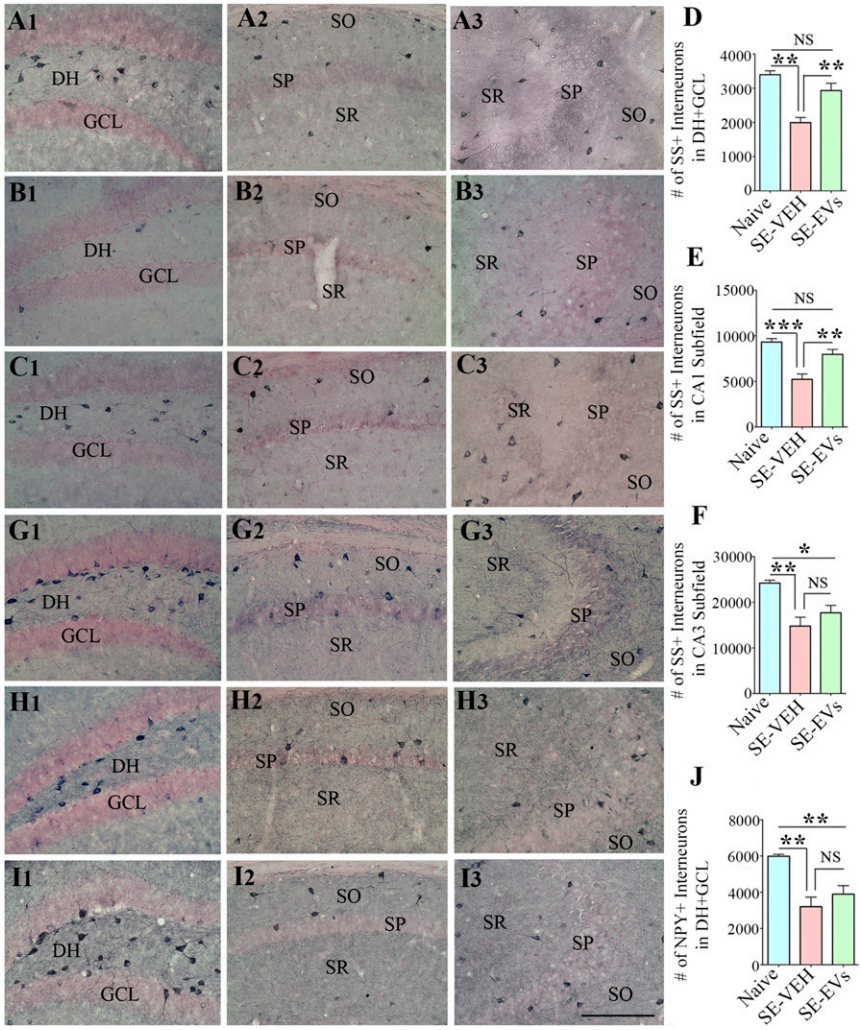

Fig. 5. IN administration of A1-exosomes 2 h after SE reduces the loss of SS^+ and NPY^+ interneurons in the hippocampus when examined 4 d post-SE. (*A1–C3*) Distribution of SS^+ interneurons in the DG (*A1*, *B1*, and *C1*), the CA1 subfield (*A2*, *B2*, and *C2*), and the CA3 subfield (*A3*, *B3*, and *C3*) of a naive control mouse (*A1–A3*), a mouse in the SE-VEH group (*B1–B3*), and a mouse in the SE-EVs group (*C1–C3*). Bar charts in *D–F* compare the numbers of SS^+ interneurons in the DH+GCL (*D*) and the CA1 and CA3 subfields (*E* and *F*) of the hippocampus. All regions display a significant loss of SS^+ interneurons in the SE-VEH group, but only the CA3 subfield shows some loss in the SE-EVs group. Overall, the SE-EVs group exhibits greater numbers of SS^+ interneurons than the SE-VEH group in all regions, implying a considerable protection after IN administration of A1-exosomes. (*G1–I3*) Distribution of NPY^+ interneurons in the DG (*G1*, *H1*, and *I1*), the CA1 subfield (*G2*, *H2*, and *I2*), and the CA3 subfield (*G3*, *H3*, and *I3*) of a naive control mouse (*G1–G3*), a mouse from the SE-VEH group (*H1–H3*), and a mouse from the SE-EVs group (*I1–I3*). Bar chart in *J* compares the numbers of NPY^+ interneurons in the DH+GCL (*I*) of the hippocampus. Although both SE groups display reduced numbers of NPY^+ interneurons in the DH+GCL in comparison with the naive control group, the SE-EVs group exhibits relatively greater numbers of PV^+ interneurons than the SE-VEH group, implying some protection of these interneurons after IN administration of A1-exosomes. SO, stratum oriens, SP, stratum pyramidale; SR, stratum radiatum (*$P < 0.05$, **$P < 0.01$, and ***$P < 0.001$). (Scale bar: 200 μm.)

(Fig. 7 *I–L*). This revealed reduced abnormal migration of newly born granule cells into the DH in animals belonging to the SE-EVs group compared with the SE-VEH group ($P < 0.05$; Fig. 7*L*). Thus, A1-exosome treatment after SE facilitated maintenance of normal pattern and extent of neurogenesis with preservation of reelin$^+$ neurons and minimal aberrant migration of newly born granule cells.

IN Delivery of A1-Exosomes After SE Led to Reduced Hippocampal Inflammation in the Chronic Phase. To examine whether A1-exosome–mediated suppression of hippocampal inflammation observed in the early phase after SE persists in the chronic phase, we examined microglia in the hippocampus through IBA-1 immunostaining 6 wk after SE (Fig. 7 *M1–Q*). Animals in the SE-VEH group exhibited enhanced density of microglia with hypertrophied soma and thick, short processes (Fig. 7 *N1–N3*). Such microglia were prominently seen in the DG and the CA1 subfield. In contrast, animals in the SE-EVs group showed highly ramified microglia (Fig. 7 *O1–O3*), akin to those seen in age-matched naive control animals (Fig. 7 *M1–M3*). Measurement of the area occupied by IBA-1–reactive elements revealed increased microglial activity in DG and CA1 regions of animals belonging to the SE-VEH group compared with the naive control group and the SE-EVs group ($P < 0.001$; $n = 4$ per group; Fig. 7 *P–Q*). Thus, A1-exosome treatment early after SE restrained hippocampal inflammation for prolonged periods.

Discussion

The present results demonstrate that IN delivery of A1-exosomes 2 h after SE onset is efficacious for reducing multiple SE-induced adverse effects in the hippocampus, a region of the brain vital for learning and memory. The beneficial effects of A1-exosome treatment in the early phase after SE comprised (*i*) suppression of SE-induced surge in multiple proinflammatory cytokines, (*ii*) enhanced expression of a few antiinflammatory cytokines and trophic factors, (*iii*) diminished activation of microglia, (*iv*) reduced loss of dentate hilar neurons (presumably comprising excitatory and inhibitory hilar neurons), (v) robust protection of glutamatergic CA1 pyramidal neurons, and (vi) reduced loss of several subclasses of GABAergic inhibitory interneurons, including those expressing the calcium binding protein PV and neuropeptides SS and NPY. The early favorable effects after SE led to maintenance of a normal pattern and extent of neurogenesis with minimal loss of reelin$^+$ interneurons, reduced aberrant migration of newly born granule cells into the DH, and diminished inflammation in the chronic phase after SE. Moreover, the extent of neuroprotective and antiinflammatory effects mediated by A1-exosome treatment was sufficient for preserving normal cognitive and memory function. Importantly, these changes were preceded by incorporation of IN-administered A1-exosomes into a large number of neurons in the frontoparietal cortex and the dorsal hippocampus, and a vast majority of microglia in rostral regions of the cortex. In addition, exosomes were frequently seen

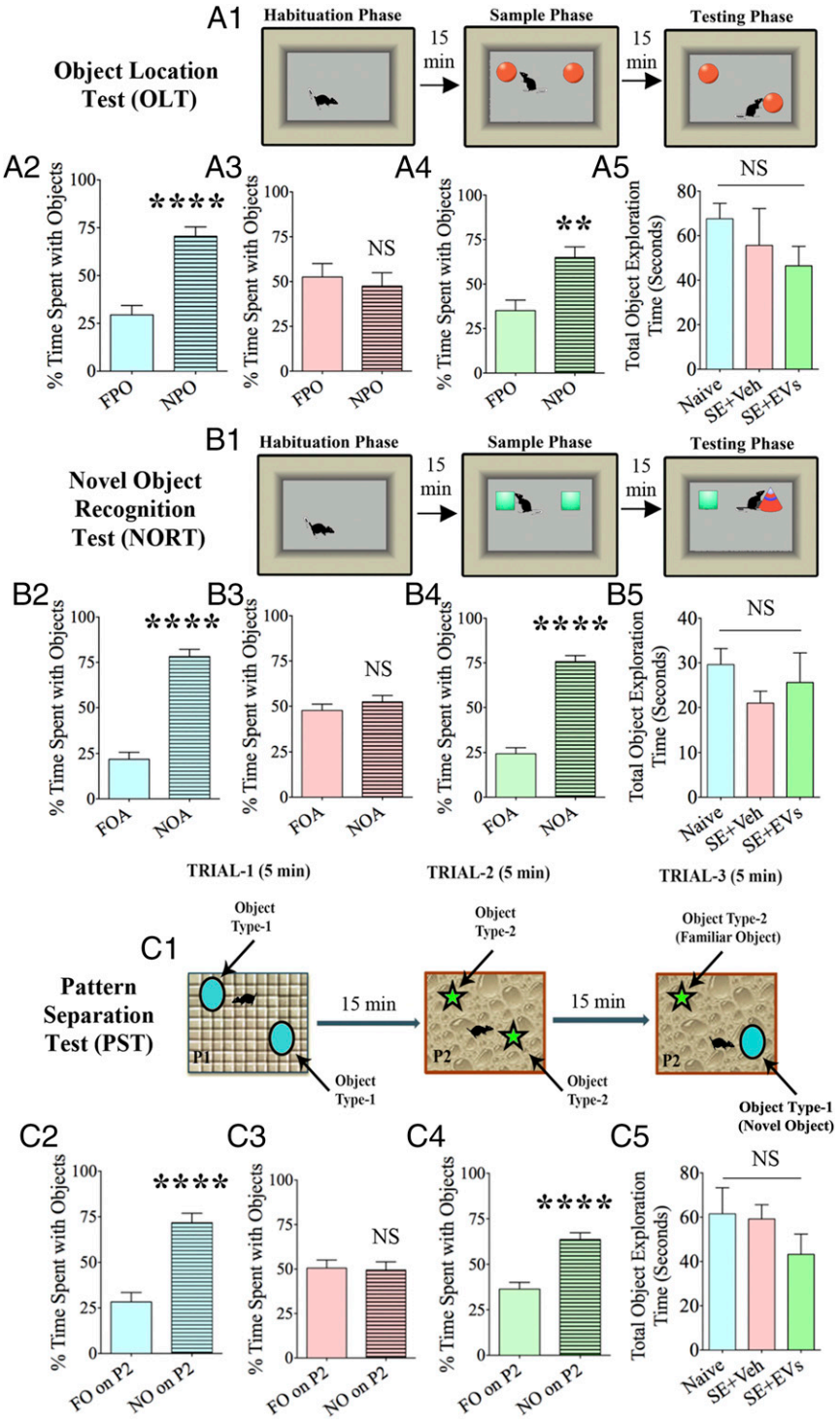

Fig. 6. IN administration of A1-exosomes after SE prevents cognitive, memory, and pattern-separation impairments. (*A1*, *B1*, and *C1*) Depiction of various phases involved in an OLT (*A1*), a NORT (*B1*), and a PST (*C1*). Bar charts in *A2–A4*, *B2–B4*, and *C2–C4* compare percentages of time spent with different objects. Naive control animals showed a greater affinity for (*i*) the NPO over the FPO in an OLT (*A2*), (*ii*) the NO area (NOA) over the FO area (FOA) in a NORT (*B2*), and (*iii*) NO on P2 over the FO on P2 in a PST (*C2*), implying normal cognitive, memory, and pattern-separation function. However, animals in the SE+VEH group were impaired in all three tests (*A3*, *B3*, and *C3*). This was evinced by their behavior of spending nearly equal amounts of the object exploration time with the FPO and the NPO in OLT (*A3*), FOA and NOA in NORT (*B3*), and FO on P2 and NO on P2 in the PST (*C3*). In contrast, animals in the SE-EVs group showed a greater affinity for exploring the NPO in OLT (*A4*), NOA in NORT (*B4*), and NO on P2 in PST (*C4*), suggesting a similar cognitive, memory, and pattern-separation function as naive control animals. Bar charts in *A5*, *B5*, and *C5* show that animals in different groups explored objects for comparable durations (**$P < 0.01$ and ****$P < 0.0001$).

adjacent to processes of astrocytes and microglia throughout the frontoparietal cortex and the hippocampus. A proinflammatory cytokine storm and loss of glutamatergic and GABAergic neurons in the early phase after SE and an abnormal and reduced neurogenesis with persistent inflammation in the chronic phase after SE are considered as epileptogenic and cognitive and memory-impairing alterations. Hence, the favorable outcomes mediated through IN administration of A1-exosomes have considerable significance for developing a therapy that eases the advancement of primary hippocampal injury into a chronic epileptic state.

Protracted and orchestrated hyperactivity of multiple populations of neurons typically lead to continuous seizures or SE, which cause excitotoxic neurodegeneration and neuroinflammation associated with an increase in the concentration of multiple proinflammatory cytokines and activation of microglia (5, 35, 36). In this study, IN treatment with A1-exosomes 2 h after SE resulted in their targeting into the hippocampus within 6 h of administration, which seemed to provide considerable protection to glutamatergic neurons and GABAergic interneurons in the hippocampus. The potential of A1-exosomes as a neurotherapeutic

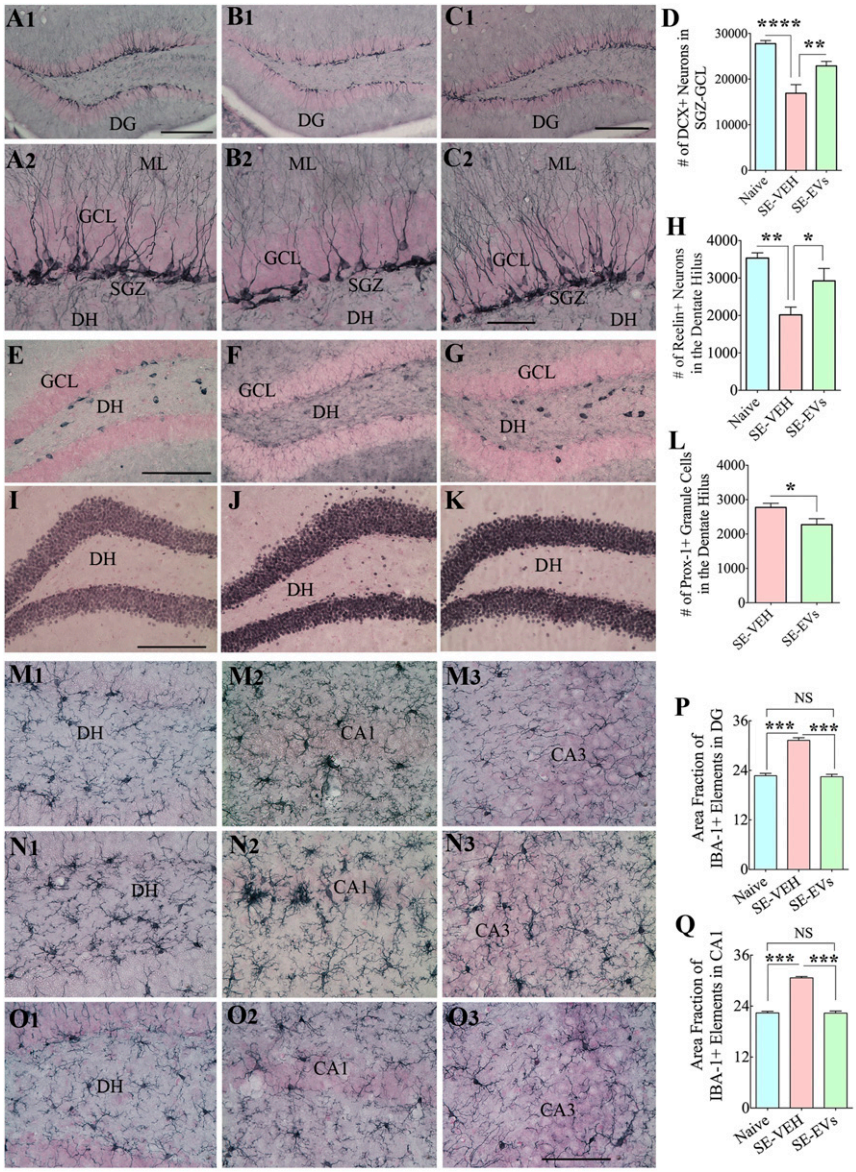

Fig. 7. IN administration of A1-exosomes 2 h after SE restrains multiple adverse changes that are typically seen in the chronic phase after SE. In comparison with naive control animals (*A1*, *A2*, *E*, *I*, and *M1–M3*), animals in the SE-VEH group showed waning of hippocampal neurogenesis [doublecortin (DCX) immunostaining; *B1* and *B2*], loss of reelin$^+$ interneurons in the DG (*F*), aberrant migration of newly born prox-1$^+$ granule cells into the DH (*J*), and persistent hippocampal inflammation (with increased density and hypertrophy of IBA-1$^+$ microglia; *N1–N3*). In animals in the SE-EVs group, the extent of neurogenesis (*C1* and *C2*), the survival of reelin$^+$ interneurons (*G*), and the morphology and density of IBA-1$^+$ microglia (*O1–O3*) were comparable to those observed in naive control animals (*A1*, *A2*, *E*, *I*, and *M1–M3*). In addition, aberrant migration of newly born cells into the DH was reduced (*K*) in these animals. ML, molecular layer. Bar charts compare numbers of DCX$^+$ newly born neurons in the SGZ-GCL (*D*), reelin$^+$ interneurons in the DH (*H*), numbers of prox-1$^+$ newly born granule cells in the DH (*L*), and IBA-1$^+$ microglia in the DG (*P*) and the CA1 subfield (*Q*) between groups. Note that the extent of neurogenesis (*D*) and numbers of reelin$^+$ interneurons (*H*) and IBA-1$^+$ structures (*P* and *Q*) in SE-EVs group animals were comparable to those seen in naive control animals. In addition, SE-EVs animals showed reduced numbers of prox-1$^+$ cells in the DH (*L*), implying a reduced abnormal migration of newly born granule cells with A1-exosome treatment after SE (*$P < 0.05$, **$P < 0.01$, ***$P < 0.001$, and ****$P < 0.0001$). (Scale bars: *A1*, *B1*, and *C1*, 200 μm; *A2*, *B2*, and *C2*, 50 μm; *E–G* and *I–K*, 200 μm; *M1–O3*, 100 μm.)

product was first discovered in a model of traumatic brain injury (TBI) when a single i.v. administration of A1-exosomes after TBI considerably suppressed inflammation and improved spatial learning and pattern separation ability (20). Nonetheless, the efficacy of these exosomes when dispensed through an IN route or in an excitotoxic injury model was unknown. In this regard, the present study provides compelling evidence that IN administration of A1-exosomes is neuroprotective when application is commenced 2 h after SE. Measurement of proinflammatory cytokines 24 h post-SE and activation of microglia 4 d post-SE revealed that IN treatment of A1-exosomes considerably eases neuroinflammation resulting from SE. This was exemplified by the reduced concentration of multiple proinflammatory cytokines, enhanced expression of a few antiinflammatory cytokines and trophic factors, and reduced occurrence of activated microglia. The proinflammatory cytokines that showed increased expression with SE and VEH treatment but reduced expression with SE and A1-exosome treatment comprised (*i*) TNF-α, a prominent cytokine secreted by activated macrophages involved in inflammation and several brain diseases; (*ii*) IL1-β, another prominent cytokine secreted by activated macrophages and involved in inflammation; (*iii*) MCP-1, a chemokine that regulates

the migration and infiltration of monocytes and macrophages; (*iv*) SCF, a cytokine involved in hematopoiesis; (*v*) MIP-1α, a protein involved in leukocyte recruitment; and (*vi*) GM-CSF, a protein that stimulates stem cells to produce granulocytes. Among these, TNF-α and IL-1β are also considered as proconvulsant cytokines because of their propensity for contributing to epileptogenesis and chronic epilepsy development after an initial injury (31).

The antiinflammatory cytokines or factors that showed enhanced expression with A1-exosome treatment include (*i*) IL-10, a well-known antiinflammatory cytokine; (*ii*) G-CSF, a factor that stimulates bone marrow to produce new blood cells; (*iii*) PDGF-β, a factor that promotes angiogenesis; (*iv*) IL-6, a cytokine that acts as a proinflammatory and antiinflammatory protein; and (*v*) IL-2, a cytokine involved in immune tolerance and immunity. Furthermore, A1-exosome treatment reduced the overall number of ED1$^+$ activated microglia in the hippocampus by 66% when examined 4 d post-SE. Additionally, examination of IBA-1$^+$ microglia at 6 wk post-SE revealed persistent inflammation in animals belonging to the SE-VEH group but not in the SE-EVs group. Greatly reduced inflammation observed after SE with A1-exosome treatment has implications because persistent inflammation is one of the key players in the evolution of neurodegenerative diseases, including temporal-lobe epilepsy (37). Indeed, enhanced concentrations of proinflammatory cytokines are constantly observed in the epileptic hippocampus (38), and are derived from activated microglia/macrophages and reactive astrocytes (38, 39). In this regard, diminished inflammation with normalization of TNF-α and IL-1β concentrations and reduced numbers of ED1$^+$ activated microglia in the SE-EVs group imply that A1-exosome treatment is effective for curbing the SE-induced inflammation cascade. Considering the robust incorporation of exosomes into microglia in rostral regions of the cortex and association of exosomes with processes of microglia and astrocytes in the hippocampus, it is plausible that antiinflammatory effects of IN administered A1-exosomes were mediated by modulation of microglia and astrocytes directly or indirectly through the release of antiinflammatory proteins.

The antiinflammatory effects of A1-exosome treatment were also accompanied by robust neuroprotection, epitomized by diminished loss of neurons in the DH and the CA1 pyramidal cell layer, two regions in the hippocampus that typically display increased vulnerability to SE-induced neuronal death (5, 40, 41). Moreover, IN administration of A1-exosomes after SE promoted preservation of subclasses of GABAergic interneurons, particularly those expressing PV and SS. This was evident in the finding of 34–69% greater numbers of these interneurons in the DG and CA1 subfield of animals in the SE-EVs group compared with animals in the SE-VEH group. Interneuron preservation has great importance because severe loss of PV$^+$ and SS$^+$ interneurons leads to chronic epilepsy typified by spontaneous recurrent seizures and cognitive and mood impairments (41–45). Neuroprotective effects were likely a consequence of robust antiinflammatory effects of exosomes. Nonetheless, some direct neuroprotective and/or neuron-reparative effects through the release of neurotrophic factors cannot be ruled out as exosomes incorporated into many neurons in the hippocampus and the frontoparietal cortex.

Another important feature of A1-exosome treatment after SE was its proficiency in maintaining a normal pattern and extent of neurogenesis for an extended period after SE and in reducing the size of aberrant neurogenesis. Animals in the SE-VEH group exhibited clearly reduced neurogenesis in the SGZ-GCL, whereas animals in the SE-EVs group presented neurogenesis that was comparable to age-matched naive control animals. Deviant neurogenesis after SE is exemplified by an anomalous migration of newly born dentate granule cells into the DH (46, 47). In the present study, such aberrant migration was ostensible in the SE-VEH group but significantly lowered in the SE-EVs group. Dampening of SE-induced aberrant neurogenesis through A1-exosome treatment has implications because deviant neurogenesis has been shown to facilitate the expansion of epileptogenic circuitry between dentate granule cells relocated to the DH and CA3 pyramidal neurons. It is currently unknown whether these anomalies by themselves are adequate to induce spontaneous seizures (48). Nonetheless, their involvement in manifestations of spontaneous seizures after SE has been well documented (49–54). We measured reelin$^+$ interneurons in the DH to identify the mechanism behind A1-exosome–mediated inhibition of aberrant neurogenesis, as migration of newly born dentate granule cells from the SGZ to GCL is steered by reelin protein secreted by reelin$^+$ interneurons in the DH, and considerable loss of these neurons fosters aberrant displacement of newly born neurons into the DH (55). Abnormally migrated prox-1$^+$ new granule cells were accompanied with a sizable loss of reelin$^+$ interneurons in the DH of animals in the SE-VEH group. In contrast, a diminished extent of aberrant neurogenesis was apparent with the salvation of reelin$^+$ interneurons in the DH of animals in the SE-EVs group. Thus, A1-exosome treatment after SE eased aberrant neurogenesis via protection of reelin$^+$ interneurons, which is likely a result of repression of inflammation facilitated by A1-exosomes. Decreased inflammation and normal levels of neurogenesis likely also contributed to the preservation of cognitive and memory function in the SE-EVs group, as inflammation and decreased neurogenesis can impair cognitive and memory function (56, 57). A series of object-based tests in the present study demonstrated the impaired ability of animals in the SE-VEH group for cognition and memory. These include inability to discern minor changes in their environment in an OLT, identifying an NO in an NORT, and pattern separation in a PST. However, animals in the SE-EVs group exhibited similar ability as age-matched naive control animals in these tests, underscoring that A1-exosome treatment shortly after SE is efficacious for preventing cognitive and memory impairments.

In summary, the results of the present study establish that IN A1-exosome treatment after the termination of 2 h of SE can considerably repress neurodegeneration, neuroinflammation, aberrant neurogenesis, and cognitive and memory impairments. The results suggest that A1-exosomes may be used clinically as an adjunct to AED therapy after SE. Although an ideal combo of AEDs would terminate an SE crisis, IN administration of A1-exosomes shortly after SE termination would help in reducing the SE-induced neurodegeneration, neuroinflammation, and cognitive and memory impairments, which in turn may considerably reduce the predilection of SE to evolve into a chronic epileptic state. In such situations, IN dispensation of prebanked A1-exosomes generated from allogenic MSCs from multiple sources may be used (28–30). There are several advantages of the use of EVs as opposed to cells. These include their ability to cross the blood–brain barrier and deliver various therapeutic factors to the brain (25, 26); amenability for engineering to package specific mRNAs, miRNAs, and proteins (26, 27); and minimal risk for developing tumors or causing thrombosis. Future studies will be focused on determining whether the extent of neuroprotective, antiinflammatory, neurogenic, cognitive, and memory-protective effects mediated by A1-exosomes is adequate to prevent the evolution of SE-induced initial precipitating injury into a chronic epileptic state.

Materials and Methods

SI Materials and Methods includes descriptions of all materials and methods used in the present study. This includes culture conditions, chromatographic isolation of EVs, timeline of various experiments, induction of SE, IN administration of A1-exosomes, tracking of PKH-26$^+$ labeled exosomes in the brain, behavioral testing procedures, immunohistochemistry for neuroinflammation and neuroprotection analyses, stereological cell-counting methods, and measurement of microglia with ImageJ software. Human bone marrow-derived MSCs were from the Center for MSC Distribution (medicine.tamhsc.edu/irm/msc-distribution.html), and the Texas A&M Animal Care and Use Committee approved all animal protocols. Human bone marrow-derived MSCs were obtained from normal, healthy donors

after informed consent in accordance with procedures approved by the Scott & White and Texas A&M Institutional Review Boards.

ACKNOWLEDGMENTS. This study was supported by Emerging Technology Funds from the State of Texas (A.K.S.); Department of Veterans Affairs Merit Award I01 BX002351 (to A.K.S.), National Institutes of Health Grant P40OD011050 (to D.J.P.), Biomedical Laboratory Research and Development (BLR&D) Research Career Scientist Award 1IK6BX003612 from the Department of Veterans Affairs (to A.K.S.), and Government of China Grant NSFC-No.31301216; 2014KJXX-29 (to Q.L.). Q.L. was a visiting research scholar from the Department of Neurosurgery, Xi'an Central Hospital, School of Medicine, Xi'an Jiao Tong University, Xi'an, P.R. China. The contents of this article suggest the views of authors and do not represent the views of the US Department of Veterans Affairs or the United States Government.

1. Seinfeld S, Goodkin HP, Shinnar S (2016) Status epilepticus. *Cold Spring Harb Perspect Med* 6:a022830.
2. Khoujah D, Abraham MK (2016) Status epilepticus: What's new? *Emerg Med Clin North Am* 34:759–776.
3. Vezzani A, Dingledine R, Rossetti AO (2015) Immunity and inflammation in status epilepticus and its sequelae: Possibilities for therapeutic application. *Expert Rev Neurother* 15:1081–1092.
4. Löscher W (2015) Single versus combinatorial therapies in status epilepticus: Novel data from preclinical models. *Epilepsy Behav* 49:20–25.
5. Mishra V, et al. (2015) Resveratrol treatment after status epilepticus restrains neurodegeneration and abnormal neurogenesis with suppression of oxidative stress and inflammation. *Sci Rep* 5:17807.
6. Shetty AK, Hattiangady B (2007) Concise review: Prospects of stem cell therapy for temporal lobe epilepsy. *Stem Cells* 25:2396–2407.
7. Hattiangady B, Shetty AK (2010) Decreased neuronal differentiation of newly generated cells underlies reduced hippocampal neurogenesis in chronic temporal lobe epilepsy. *Hippocampus* 20:97–112.
8. Ben-Ari Y (2012) Blocking seizures with the diuretic bumetanide: Promises and pitfalls. *Epilepsia* 53:394–396.
9. Loscher W (2012) Strategies for antiepileptogenesis: Antiepileptic drugs versus novel approaches evaluated in post-status epilepticus models of temporal lobe epilepsy. *Jasper's Basic Mechanisms of the Epilepsies*, eds Noebels JL, Avoli M, Rogawski MA, Olsen RW, Delgado-Escueta AV (National Center for Biotechnology Information, Bethesda, MD), 4th Ed, pp 1055–1065.
10. Sankar R, Mazarati A (2012) Neurobiology of depression as a comorbidity of epilepsy. *Jasper's Basic Mechanisms of the Epilepsies*, eds Noebels JL, Avoli M, Rogawski MA, Olsen RW, Delgado-Escueta AV (National Center for Biotechnology Information, Bethesda, MD), 4th Ed, pp 945–956.
11. Shetty AK (2014) Hippocampal injury-induced cognitive and mood dysfunction, altered neurogenesis, and epilepsy: Can early neural stem cell grafting intervention provide protection? *Epilepsy Behav* 38:117–124.
12. Varvel NH, et al. (2016) Infiltrating monocytes promote brain inflammation and exacerbate neuronal damage after status epilepticus. *Proc Natl Acad Sci USA* 113:E5665–E5674.
13. Sahin M, Menache CC, Holmes GL, Riviello JJ (2001) Outcome of severe refractory status epilepticus in children. *Epilepsia* 42:1461–1467.
14. Temkin NR (2001) Antiepileptogenesis and seizure prevention trials with antiepileptic drugs: Meta-analysis of controlled trials. *Epilepsia* 42:515–524.
15. Dichter MA (2009) Emerging concepts in the pathogenesis of epilepsy and epileptogenesis. *Arch Neurol* 66:443–447.
16. Trinka E, Kälviäinen R (2017) 25 years of advances in the definition, classification and treatment of status epilepticus. *Seizure* 44:65–73.
17. Sloviter RS, Bumanglag AV (2013) Defining "epileptogenesis" and identifying "antiepileptogenic targets" in animal models of acquired temporal lobe epilepsy is not as simple as it might seem. *Neuropharmacology* 69:3–15.
18. Patterson V, Pant P, Gautam N, Bhandari A (2014) A Bayesian tool for epilepsy diagnosis in the resource-poor world: development and early validation. *Seizure* 23:567–569.
19. Agadi S, Shetty AK (2015) Concise review: Prospects of bone marrow mononuclear cells and mesenchymal stem cells for treating status epilepticus and chronic epilepsy. *Stem Cells* 33:2093–2103.
20. Kim DK, et al. (2016a) Chromatographically isolated CD63+CD81+ extracellular vesicles from mesenchymal stromal cells rescue cognitive impairments after TBI. *Proc Natl Acad Sci USA* 113:170–175.
21. Salem HK, Thiemermann C (2010) Mesenchymal stromal cells: Current understanding and clinical status. *Stem Cells* 28:585–596.
22. Phinney DG, et al. (2015) Mesenchymal stem cells use extracellular vesicles to outsource mitophagy and shuttle microRNAs. *Nat Commun* 6:8472.
23. Heldring N, Mäger I, Wood MJ, Le Blanc K, Andaloussi SE (2015) Therapeutic potential of multipotent mesenchymal stromal cells and their extracellular vesicles. *Hum Gene Ther* 26:506–517.
24. Anderson JD, et al. (2016) Comprehensive proteomic analysis of mesenchymal stem cell exosomes reveals modulation of angiogenesis via nuclear factor-kappaB signaling. *Stem Cells* 34:601–613.
25. Cossetti C, et al. (2014) Extracellular vesicles from neural stem cells transfer IFN-γ via Ifngr1 to activate Stat1 signaling in target cells. *Mol Cell* 56:193–204.
26. Batrakova EV, Kim MS (2015) Using exosomes, naturally-equipped nanocarriers, for drug delivery. *J Control Release* 219:396–405.
27. EL Andaloussi S, Mäger I, Breakefield XO, Wood MJ (2013) Extracellular vesicles: Biology and emerging therapeutic opportunities. *Nat Rev Drug Discov* 12:347–357.
28. Kimbrel EA, et al. (2014) Mesenchymal stem cell population derived from human pluripotent stem cells displays potent immunomodulatory and therapeutic properties. *Stem Cells Dev* 23:1611–1624.
29. Watson N, et al. (2015) Discarded Wharton jelly of the human umbilical cord: A viable source for mesenchymal stromal cells. *Cytotherapy* 17:18–24.
30. Lim MH, Ong WK, Sugii S (2014) The current landscape of adipose-derived stem cells in clinical applications. *Expert Rev Mol Med* 16:e8.
31. Li G, et al. (2011) Cytokines and epilepsy. *Seizure* 20:249–256.
32. Hattiangady B, et al. (2014) Object location and object recognition memory impairments, motivation deficits and depression in a model of Gulf War illness. *Front Behav Neurosci* 8:78.
33. Yassa MA, Stark CE (2011) Pattern separation in the hippocampus. *Trends Neurosci* 34:515–525.
34. Leutgeb JK, Leutgeb S, Moser MB, Moser EI (2007) Pattern separation in the dentate gyrus and CA3 of the hippocampus. *Science* 315:961–966.
35. Wasterlain CG, Naylor DE, Liu H, Niquet J, Baldwin R (2013) Trafficking of NMDA receptors during status epilepticus: Therapeutic implications. *Epilepsia* 54:78–80.
36. Janigro D, Iffland PH, 2nd, Marchi N, Granata T (2013) A role for inflammation in status epilepticus is revealed by a review of current therapeutic approaches. *Epilepsia* 54:30–32.
37. Amor MM, Eltawansy SA, Osofsky J, Holland N (2014) Recurrent sinus pauses: An atypical presentation of temporal lobe epilepsy. *Case Rep Crit Care* 2014:918247.
38. Vezzani A (2013) Fetal brain inflammation may prime hyperexcitability and behavioral dysfunction later in life. *Ann Neurol* 74:1–3.
39. Prinz M, Priller J (2014) Microglia and brain macrophages in the molecular age: From origin to neuropsychiatric disease. *Nat Rev Neurosci* 15:300–312.
40. Rao MS, Hattiangady B, Reddy DS, Shetty AK (2006) Hippocampal neurodegeneration, spontaneous seizures, and mossy fiber sprouting in the F344 rat model of temporal lobe epilepsy. *J Neurosci Res* 83:1088–1105.
41. Hattiangady B, Kuruba R, Shetty AK (2011) Acute seizures in old age leads to a greater loss of CA1 pyramidal neurons, an increased propensity for developing chronic TLE and a severe cognitive dysfunction. *Aging Dis* 2:1–17.
42. Vezzani A, Sperk G, Colmers WF (1999) Neuropeptide Y: Emerging evidence for a functional role in seizure modulation. *Trends Neurosci* 22:25–30.
43. Schwaller B, et al. (2004) Parvalbumin deficiency affects network properties resulting in increased susceptibility to epileptic seizures. *Mol Cell Neurosci* 25:650–663.
44. Houser CR (2014) Do structural changes in GABA neurons give rise to the epileptic state? *Adv Exp Med Biol* 813:151–160.
45. Murray AJ, et al. (2011) Parvalbumin-positive CA1 interneurons are required for spatial working but not for reference memory. *Nat Neurosci* 14:297–299.
46. Parent JM, et al. (1997) Dentate granule cell neurogenesis is increased by seizures and contributes to aberrant network reorganization in the adult rat hippocampus. *J Neurosci* 17:3727–3738.
47. Hattiangady B, Rao MS, Shetty AK (2004) Chronic temporal lobe epilepsy is associated with severely declined dentate neurogenesis in the adult hippocampus. *Neurobiol Dis* 17:473–490.
48. Cho KO, et al. (2015) Aberrant hippocampal neurogenesis contributes to epilepsy and associated cognitive decline. *Nat Commun* 6:6606.
49. Kuruba R, Hattiangady B, Shetty AK (2009) Hippocampal neurogenesis and neural stem cells in temporal lobe epilepsy. *Epilepsy Behav* 14:65–73.
50. Scharfman HE, Goodman JH, Sollas AL (2000) Granule-like neurons at the hilar/CA3 border after status epilepticus and their synchrony with area CA3 pyramidal cells: Functional implications of seizure-induced neurogenesis. *J Neurosci* 20:6144–6158.
51. Scharfman HE, Sollas AL, Smith KL, Jackson MB, Goodman JH (2002) Structural and functional asymmetry in the normal and epileptic rat dentate gyrus. *J Comp Neurol* 454:424–439.
52. Scharfman HE, Sollas AL, Berger RE, Goodman JH (2003) Electrophysiological evidence of monosynaptic excitatory transmission between granule cells after seizure-induced mossy fiber sprouting. *J Neurophysiol* 90:2536–2547.
53. McCloskey DP, Hintz TM, Pierce JP, Scharfman HE (2006) Stereological methods reveal the robust size and stability of ectopic hilar granule cells after pilocarpine-induced status epilepticus in the adult rat. *Eur J Neurosci* 24:2203–2210.
54. Hester MS, Danzer SC (2014) Hippocampal granule cell pathology in epilepsy - A possible structural basis for comorbidities of epilepsy? *Epilepsy Behav* 38:105–116.
55. Gong C, Wang TW, Huang HS, Parent JM (2007) Reelin regulates neuronal progenitor migration in intact and epileptic hippocampus. *J Neurosci* 27:1803–1811.
56. Ryan SM, Nolan YM (2016) Neuroinflammation negatively affects adult hippocampal neurogenesis and cognition: can exercise compensate? *Neurosci Biobehav Rev* 61:121–131.
57. Mendelsohn AR, Larrick JW (2016) Pharmaceutical rejuvenation of age-associated decline in spatial memory. *Rejuvenation Res* 19:521–524.
58. Kim DK, et al. (2016a) Scalable production of a multifunctional protein (TSG-6) that aggregates with itself and the CHO cells that synthesize it. *PLoS One* 11:e0147553.
59. Cunningham M, et al. (2014) hPSC-derived maturing GABAergic interneurons ameliorate seizures and abnormal behavior in epileptic mice. *Cell Stem Cell* 15:559–573.
60. Chen X, et al. (2016) A reduced susceptibility to chemoconvulsant stimulation in adenylyl cyclase 8 knockout mice. *Epilepsy Res* 119:24–29.
61. Shibley H, Smith BN (2002) Pilocarpine-induced status epilepticus results in mossy fiber sprouting and spontaneous seizures in C57BL/6 and CD-1 mice. *Epilepsy Res* 49:109–120.
62. Racine RJ (1972) Modification of seizure activity by electrical stimulation. II. Motor seizure. *Electroencephalogr Clin Neurophysiol* 32:281–294.
63. Rao MS, Shetty AK (2004) Efficacy of doublecortin as a marker to analyse the absolute number and dendritic growth of newly generated neurons in the adult dentate gyrus. *Eur J Neurosci* 19:234–246.